www.elsevier.nl/locate/jorganchem

Journal of Organometallic Chemistry 589 (1999) 2–10

Organometallic iridium(III) and rhenium(I) complexes with lumazine, alloxazine and pterin derivatives

Oliver Heilmann [a], Fridmann M. Hornung [a], Jan Fiedler [b], Wolfgang Kaim [a,*]

[a] *Institut für Anorganische Chemie der Universität, Pfaffenwaldring 55, D-70550 Stuttgart, Germany*
[b] *J. Heyrovsky Institute of Physical Chemistry, Academy of Sciences of the Czech Republic, Dolejškova 3, CZ-18223 Prague, Czech Republic*

Received 24 February 1999

Abstract

Two organometallic complex fragments with $5d^6$ configurated metal centres of different character, electrophilic $[Ir^{III}Cp^*Cl]^+$ and π-donating $[Re^I(CO)_3Cl]$, were used as probes in compounds containing 1,3-dimethyllumazine (DML), 1,3-dimethylalloxazine (DMA), 2-pivaloylpterin (PP) and 6-methyl-2-pivaloylpterin (MPP) as biochemically relevant ligands. Evidence from spectroscopy (NMR, IR, UV–vis) in aprotic solvents points in most cases to the O4 and N5 atoms as chelate donors for metal binding. For $[(DMA)Ir^{III}Cp^*Cl](PF_6)$ this was substantiated by a crystal structure analysis. With PP, however, an iridium(III) compound with pivaloyl-coordinated metal was obtained. Whereas both the Ir^{III} and Re^I complexes of the good π acceptor ligand DMA can be reduced reversibly and thus studied by (spectro)electrochemistry (IR, UV–vis, EPR: ligand-centred one-electron reduction), the DML system exhibits such behaviour only for the Ir^{III} species. The complexes of the 2-pivaloylpterins showed only irreversible reduction.

Keywords: Electrochemistry; Electron paramagnetic resonance (EPR); Iridium; Rhenium; Spectroscopy

1. Introduction

As heterocycles related to the biochemically ubiquitous coenzymes of the flavin and tetrahydropterin family, the substituted or unsubstituted lumazines, alloxazines and pterins have attracted interest not only in organic and physicochemical studies but also as potential ligands in coordination chemistry [1–3].

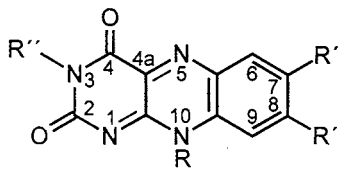

flavin

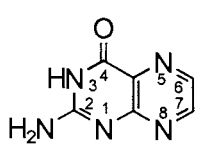

pterin

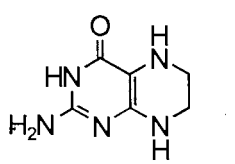

5,6,7,8-tetrahydropterin

Recent reviews of this subject have summarised the possible relevance of such complexes for biological electron transfer [2] and the structural results from a number of crystallographically characterised compounds [1].

Although organometallic complex fragments such as $[Cp^*M]^{2+}$ or $[Cp^*ClM]^+$ ($Cp^* = C_5Me_5$, M = Rh, Ir) are known to be suitable probes for biorelevant ligands like nucleic acids or amino acids in aqueous or non-aqueous media [4–11], there have been only a few studies involving the ligands mentioned above. Using 1,3-dimethylated lumazine (DML) and alloxazine (DMA), we have previously described the complexes $(DML)Re(CO)_3Cl$ [12], $[(DML)MCp^*Cl](PF_6)$ (crystal structures for both M = Rh, Ir) [13,14] and $[(DMA)Ir^{III}Cp^*Cl](PF_6)$ [14]; however, no organometallic compound of a pterin derivative has been reported to date. The alloxazine [15–18] ligand differs from the isoalloxazine system of the flavins [1,3] by substitution at N1 instead of N10. In this work we use 2-pivaloylpterin (PP) and 6-methyl-2-pivaloylpterin (MPP) as pterin [19] ligands that are sufficiently soluble

* Corresponding author.

0022-328X/99/$ - see front matter
PII: S0022-328X(99)00294-6

in aprotic media through the prevention of intermolecular hydrogen bonding involving the NH_2 group in the 2-position [20]. Studies in aprotic media are justified by the frequent occurrence of hydrophobic domains within proteins, often associated with the active site or inner membrane regions. Alkyl substitution in the 6-position of pterins is biochemically relevant regarding e.g. folic acid [1]. Spectroscopy (NMR, IR, UV–vis) and (spectro)electrochemistry in such solvents have been used for the characterisation and for the study of electron-transfer behaviour of compounds between DML, DMA, PP or MPP with $[Re^{I}(CO)_3Cl]$ or pentamethylcyclopentadienyliridium(III) species as organometallic complex fragments. The former contains a π-electron-donating $5d^6$ carbonylmetal centre in a relatively low oxidation state, which may give rise to low-lying metal-to-ligand charge transfer transitions [21–24], whereas the cationic Ir^{III} species (also $5d^6$ configuration) exhibit no such characteristics [14,25–27]. Coordination compounds of both kinds of fragments with α-diimine chelate ligands have been well researched due to the particular photo- and electrochemical behaviour [21–29].

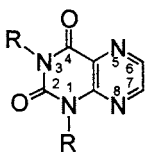

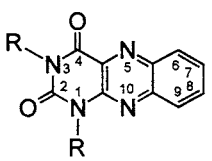

R = CH_3: DML DMA

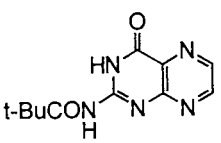

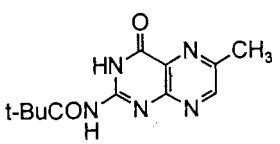

PP MPP

Although the O4–N5 chelate coordination of the DML, DMA and pterin ligands may be expected [1], this binding mode is established here for an alloxazin derivative, viz. $[(DMA)Ir^{III}Cp^*Cl](PF_6)$ by a crystal structure analysis. We shall, however, demonstrate that the less π-accepting but more acidic pterin system can provide a different coordination site for the binding of electrophilic Ir^{III}.

2. Results and discussion

2.1. Synthesis and basic characterization

The new complexes described in this study were obtained by reactions between $Re(CO)_5Cl$ or $[IrCp^*Cl(S)_2](PF_6)$ and the respective ligands (S = solvent molecule, i.e. CH_3OH or acetone). The latter was obtained by treating $(IrCp^*Cl_2)_2$ [30] with two equivalents of $AgPF_6$ in the solvent S. Reaction of PP with $[IrCp^*Cl(acetone)_2](PF_6)$ required prolonged heating and column chromatography on Al_2O_3 which resulted in the loss of HCl and the formation of a species $[(PP–H^+)IrCp^*](PF_6)$ with pivaloyl-coordinated metal and deprotonated PP (cf. below). Rhodium(III) analogues of the iridium species could be isolated only for the DML ligand system [13].

Analyses of ^{1}H-NMR and IR spectra confirmed the purity and identity of the compounds (see Section 3). The chemical shifts to lower field relative to the free ligands and the carbonyl stretching patterns suggest coordination of the 14-valence-electron fragments $[Ir^{III}Cp^*Cl]^+$ and $[fac\text{-}Re^{I}(CO)_3Cl]$ through the O4 and N5 atoms of the ligands, except for the PP/Ir^{III} combination. Most characteristic of this is the low-energy shift and IR absorption intensity reduction of the carbonyl stretching band associated with C4–O4 for the O4/N5 bonded complexes (see Table 4). This effect results from a slightly decreased bond order through metal binding at O4 and through a diminished dipole moment change of the C4–O4 vibration. On the other hand, the bands attributed to the C2–O2 vibration in DML or DMA ligands or the pivaloyl carbonyl group in $(L)Re(CO)_3Cl$, L = PP or MPP, are shifted slightly to higher energies. For compound $[(PP–H^+)IrCp^*](PF_6)$ the reverse is found, a low-energy shift of the pivaloyl carbonyl stretching band and a high-energy shift of ν(C4–O4). We tentatively suggest an arrangement **A** or **B** with precedent from other complexes of deprotonated pterin ligands [1,31] and from the well-established bioorganometallic chemistry of $[Cp^*M]^{2+}$ [4–11]. The high-field shifted ^{1}H-NMR resonances in comparison to neutral $(PP)Re(CO)_3Cl$ support the presence of a deprotonated PP ligand.

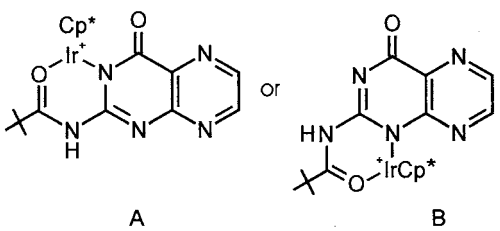

A B

2.2. Molecular and crystal structure of [(DMA)IrCp* Cl](PF6)

Following the successful growth of single crystals we can report here the first structural study of a simple alloxazine metal complex [15–17]. Compound $[(DMA)IrCp^*Cl](PF_6)$ was crystallized by slow evaporation of an acetone solution. The main results of the structural analysis are summarized in Table 1; Fig. 1 shows the view of one ion pair with atomic numbering.

Table 1
Selected bond parameters of [(DMA)IrCp*Cl](PF_6) [a]

Bond distances (Å)	
Ir(1)–N(13)	2.138(4)
Ir(1)–O(2)	2.200(4)
Ir(1)–Cl(1)	2.370(2)
Ir(1)–C(3)	2.150(6)
Ir(1)–C(4)	2.142(5)
Ir(1)–C(5)	2.156(6)
Ir(1)–C(6)	2.163(6)
Ir(1)–C(7)	2.168(5)
C(13)–O(2)	1.247(6)
N(13)–C(12)	1.330(6)
C(12)–C(13)	1.450(8)
C(11)–O(1)	1.214(7)
Bond angles (°)	
N(13)–Ir(1)–O(2)	75.2(2)
N(13)–Ir(1)–Cl(1)	85.80(11)
O(2)–Ir(1)–Cl(1)	88.11(12)
Ir(1)–O(2)–C(13)	113.9(4)
Ir(1)–N(13)–C(12)	114.8(4)
N(13)–C(12)–C(13)	116.1(4)
O(2)–C(13)–C(12)	119.4(4)

[a] Note that the crystallographic numbering (in parentheses, Fig. 1) differs from the numbering according to the nomenclature for heterocycles.

(Note that the crystallographic numbering (in parentheses, Fig. 1) differs from the numbering according to the nomenclature for heterocycles.)

There are no specific intermolecular interactions, and the coordination at the metal centre is similar to that in other complex ions $[(L)IrCp^*Cl]^+$ [14,26]. The π-conjugated alloxazine ligand, which differs from the related isoalloxazine system of the flavins by substitution at N1 instead of N10, is essentially coplanar with the five-membered chelate ring involving the metal. This chelate arrangement is fairly symmetrical, the Ir–O4 (Ir(1)–O(2)) and Ir–N5 (Ir(1)–N(13)) bond lengths being slightly longer than those in the related [(DML)IrCp*Cl](PF_6) (2.186(3) and 2.103(4) Å [14]). The latter may be caused by repulsive forces between the organometallic 14 VE fragment and the proton H6 (H(15)) in the *peri* position.

It should be noted that the metal centres in the iridium(III) and rhenium(I) compunds are chiral due to ligand asymmetry. All structurally characterized complex cations $[(L)MCp^*Cl]^+$ (L = DML, DMA) crystallize as pairs of enantiomers in $P2_1/n$ with $Z = 4$ [13,14].

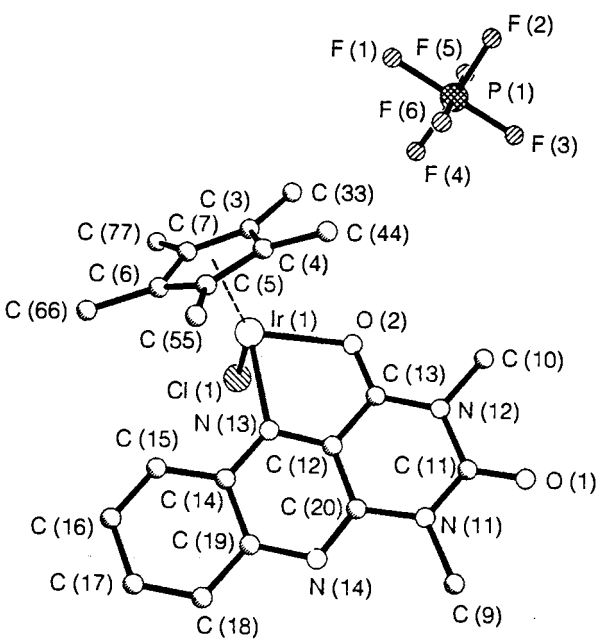

Fig. 1. Molecular structure of a [(DMA)IrCp*Cl](PF_6) ion pair in the crystal.

2.3. Cyclic voltammetry

The reducibility of the heterocyclic π systems of flavins and pterins is essential for their biological functions as coenzymes of oxidoreductases [1–3]. Similarly, the cyclic voltammetry experiments presented here for THF solutions (Table 2, Fig. 2) show that all ligands employed here can be reduced at potentials less negative than −2 V versus the ferrocenium/ferrocene couple. However, only DMA is reduced *reversibly* at the standard scan rate of 100 mV s^{-1}, owing to the better delocalization of the added charge over a larger π system. For the same reason, this ligand and its complexes are also easier reduced than the respective PP, MPP or DML analogues (Table 2).

As a general rule, metal σ coordination to π systems facilitates their reducibility, both in terms of less negative potentials and improved reversibility [21–27].

Table 2
Reduction potentials from cyclic voltammetry [a]

Compound	E_{pc}(red) [b]	Solvent [c] (reference)
DMA	−1.68(rev) [b], −2.33	THF [14]
PP	−1.83	THF
MPP	−1.77	DCE [d]
DML	−1.98	THF [14]
(DMA)Re(CO)$_3$Cl	−0.85(rev) [b], 1.73(rev) [b], −2.73	THF
(PP)Re(CO)$_3$Cl	−1.00	THF
(MPP)Re(CO)$_3$Cl	−1.02	DCE [d]
(DML)Re(CO)$_3$Cl	−1.06 [e]	DCE [d] [12]
[(DMA)IrCp*Cl](PF_6)	−0.78(rev) [b], −1.32	THF [14]
[(DML)IrCp*Cl](PF_6)	−1.05(rev) [b], −1.63	THF [14]
[(PP–H$^+$)IrCp*](PF_6)	−1.61	THF

[a] At 100 mV s^{-1} scan rate.
[b] Cathodic peak potentials in V vs. $[Fe(C_5H_5)_2]^{+/o}$; (rev) indicates electrochemically reversible process.
[c] Electrolyte 0.1 M Bu_4NPF_6.
[d] 1,2-Dichloroethane.
[e] Converted from value vs. SCE.

However, in the present case there is a variety of different responses according to the ligand used.

As expected, both Ir^{III} and Re^{I} complexes of DMA are reduced reversibly by one electron, the cationic iridium system at slightly less negative potentials than the neutral rhenium complex. For the following electron uptake the two chloride-containing species differ. Whereas the iridium compound shows an established [25–27,29] irreversible behaviour due to halide dissociation, the rhenium system still exhibits a second reversible one-electron reduction (Fig. 2). Only the third electron leads to a rapid loss of chloride [24] and irreversible behaviour.

In the case of the DML complexes, the Re^{I} compound was shown to undergo irreversible reduction [12] while the Ir^{III} complex showed reversible one-electron reduction to a neutral radical species [14].

With PP or MPP as ligand, the Re^{I} complexes are reduced in irreversible fashion, however, the less negative potentials confirm the effect of O4/N5 coordinated metal on the ligand π system. Electron paramagnetic resonance (EPR) studies of such ligands have generally shown that the lowest unoccupied MO (LUMO) is centered in the pyrazine ring [32]. In contrast, compound $[(PP–H^{+})IrCp^{*}](PF_6)$ is reduced at a rather negative potential close to that of the free ligand which supports the binding of the metal at the peripheral pivaloyl group.

2.4. Electron paramagnetic resonance spectroscopy

The EPR characteristics of the one-electron-reduced iridium(III) complexes with DML and DMA have been described [14]. Such species can be generated through cathodic reduction or from the reaction with one-electron reductants such as cobaltocene. For $[(DMA)IrCp^{*}Cl]^{\bullet}$ the latter method yielded an improved EPR resolution (Fig. 3), whereas the electrochemical in situ reduction procedure was used to study the EPR spectrum of $[(DMA)Re(CO)_3Cl]^{\bullet -}$ (Fig. 4).

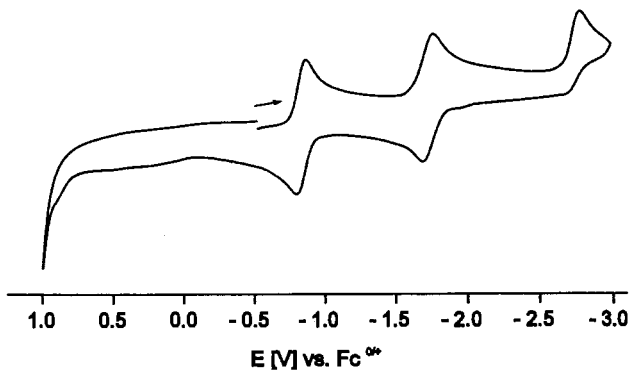

Fig. 2. Cyclic voltammogram of $(DMA)Re(CO)_3Cl$ in THF/0.1 M Bu_4NPF_6 at 100 mV s^{-1}.

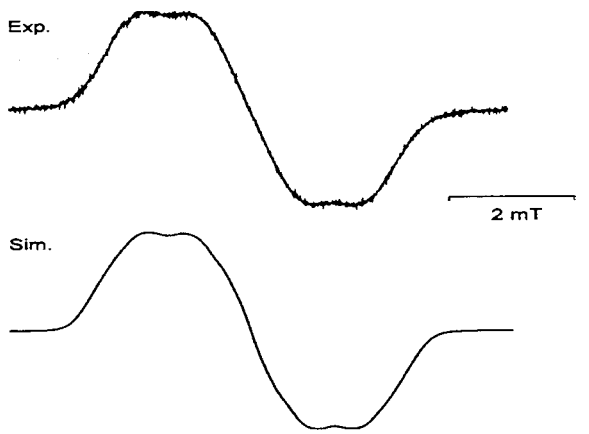

Fig. 3. EPR spectrum of $[(DMA)IrCp^{*}Cl]^{\bullet}$, generated from reduction with $CoCp_2$ in THF (top) with computer simulated spectrum (bottom; linewidth 0.15 mT).

These two paramagnetic species are clearly DMA anion radical complexes with ligand and, in particular, pyrazine ring-centred spin. In fact, the experimental and calculated [32,33] spin distributions in $DMA^{\bullet -}$ and flavosemiquinone anions are quite similar.

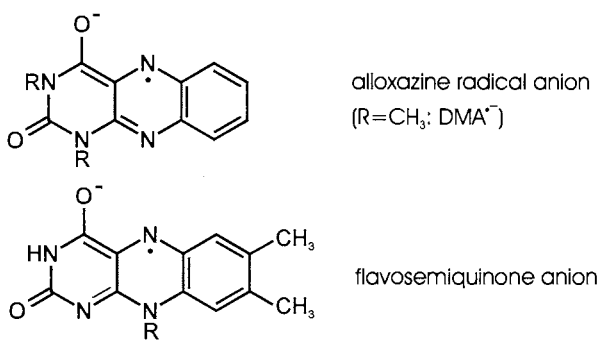

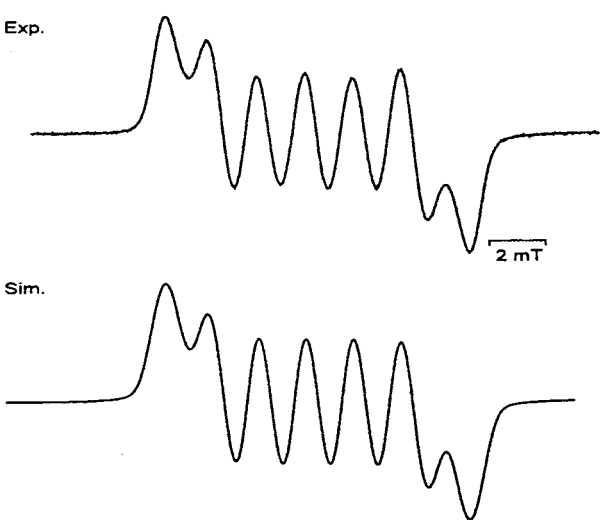

Fig. 4. EPR spectrum of $[(DMA)Re(CO)_3Cl]^{\bullet -}$ in THF/0.1 M Bu_4NPF_6 (top) with computer simulated spectrum (bottom; linewidth 1.0 mT).

Table 3
EPR data of radicals [a]

Radical	g	a_{N5}	a_{N10}	a_{H6}	a_{H9}	a_M [f]	a_M/a_0 [f]
$DMA^{\bullet -}$ [b]	2.0035	0.64	0.33	0.33	0.33		
$[(DMA)IrCp^*Cl]^{\bullet}$ [c]	1.9884	0.64	0.33	0.33	0.33	0.69 (^{193}Ir)	0.56%
	0.65 (^{191}Ir)						
$[(DMA)IrCp^*Cl]^{\bullet}$ [d]	1.9887	0.71	0.33	0.33	0.33	0.69 (^{193}Ir)	0.56%
	0.65 (^{191}Ir)						
$[(DMA)Re(CO)_3Cl]^{\bullet -}$ [e]	2.0036	0.78 [e]	Not resolved		1.68 (^{187}Re)	0.13%	
	1.66 (^{185}Re)						

[a] Hyperfine coupling constants a in mT, spectra recorded at 298 K.
[b] From chemical reduction with K in THF.
[c] From electrochemical reduction in CH_2Cl_2/0.1 M Bu_4NPF_6.
[d] From chemical reduction with $Co(C_5H_5)_2$ in THF.
[e] From electrochemical reduction in THF//0.1 M Bu_4NPF_6.
[f] For isotopic properties see main text.

Despite the predominantly ligand-centred spin, the presence of the 5d metals with large spin–orbit coupling constants and attached chloride substituents is manifested in relatively large linewidths and detectable metal isotope hyperfine splitting (^{191}Ir: 37.3% natural abundance, $I = 3/2$, $a_0 = 112.96$ mT; ^{193}Ir: 62.7%, $I = 3/2$, $a_0 = 124.60$ mT; ^{185}Re: 37.1%, $I = 5/2$, $a_0 = 1253.60$ mT; ^{187}Re: 62.9%, $I = 5/2$, $a_0 = 1266.38$ mT [34]). The coupling constants (Table 3) as obtained from simulated spectra (Figs. 3 and 4) can be set in relation to the isotropic hyperfine coupling a_0 [34] of the respective isotopes (Table 3) which shows significantly stronger spin delocalization to the iridium(III) than to the rhenium(I) centre. This is confirmed by the less pronounced g factor deviation of the rhenium radical system from the free electron value of $g = 2.0023$.

2.5. Spectroelectrochemistry in the IR region

Additional information on the effect and location of electron addition in reversibly reducible compounds can be obtained from the spectroelectrochemical analysis of vibrational bands. The carbonyl stretching region is particularly suited for such analysis as the transition $[(DMA)Re(CO)_3Cl]^{(0)\rightarrow(-)}$ illustrates (Fig. 5, Table 4), these studies have been performed on reversible couples (isosbestic points) using an optically transparent thin-layer electrolytic (OTTLE) cell [35].

Remarkably, the typical low-energy shifts on reduction are of quite comparable magnitude for the two ligand carbonyl and the three metal carbonyl bands (Table 4), which renders this method less useful for determining the spin location [36]. Similarly, the rhenium(I) and iridium(III) systems do not differ significantly, in contrast to the EPR results. However, an obvious special effect is the diminished intensity of ν(C4–O4) on reduction (Fig. 5) which again reflects the metal coordination.

2.6. UV–vis absorption spectroscopy, including solvatochromism and (spectro)electrochemistry

Although all complexes described here are coloured, their absorption in the visible part of the spectrum (cf. Fig. 6) has different origins. The rhenium(I) complexes exhibit typically intense and solvatochromic long-wavelength metal-to-ligand charge transfer (MLCT) transitions from the metal d_π to the lowest lying ligand π^* orbital [21–24,28]. These bands experience an hypsochromic shift on going from complexes of easier reducible ligands such as DMA to those of more electron rich ligands such as PP and especially MPP (Table 5). It may be noted that complexes $(L)Re(CO)_3Cl$ with L = lumiflavin and riboflavin have been described and studied [37,38] with solvent-dependent absorption maxima in a similar spectral region as those of the related $(DMA)Re(CO)_3Cl$.

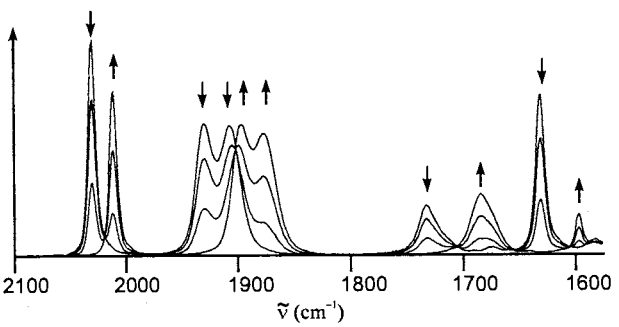

Fig. 5. Spectroelectrochemical response for the transition $[(DMA)Re(CO)_3Cl]^{(0)\rightarrow(-)}$ in the mid-infrared region (CH_3CN/0.1 M Bu_4NPF_6).

Table 4
Carbonyl stretching frequencies $\nu(cm^{-1})$ of ligands and complexes [a]

Compound	C4=O4	C2=O2	Other
DMA	1681 m	1712 vs	–
(DMA)$Re_3(CO)_3Cl$	1631 vs	1732 s	2031, 1932, 1907 (all vs) [b]
$[(DMA)Re_3(CO)_3Cl]^{\bullet -}$	1597 m	1683 s	2011, 1896, 1877 (all vs) [b]
$[(DMA)IrCp^*Cl](PF_6)$	1626 vs	1736 m	–
$[(DMA)IrCp^*Cl]^{\bullet}$	1600 w	1683 m	–
PP	1719 vs/ 1693 vs [c,e]		1625 vs [d]
	1692 sh/ 1679 vs [e,f]		1613 vs [d,f]
MPP [c]	1718 vs/ 1689 [e]		1625 vs [d]
$(PP)Re(CO)_3Cl$ [c]	1694 m		1637 vs [d]
$(MPP)Re(CO)_3Cl$ [c]	1704 m		1629 vs [d]
$[(PP–H^+)IrCp^*](PF_6)$ [f]	1710 m [f]		1595 vs [f]

[a] All DMA compounds in CH_2Cl_2 solution.
[b] Metal carbonyl ligands.
[c] In CH_2Cl_2 solution.
[d] Pivaloyl group.
[e] Tautomeric forms.
[f] In KBr.

In agreement with many other complexes of $Re(CO)_3Cl$ with π-accepting heterocyclic ligands [21–24,28], the two new rhenium(I) compounds described here show a noticable negative solvatochromism of the MLCT band, i.e. hypsochromically shifted absorption maxima in increasingly polar solvents. The λ_{max} values (in nm) for $(L)Re(CO)_3Cl$ complexes are for L = DMA (PP): 509 (467) in CH_2Cl_2, 503 (451) in THF, 478 (423) in acetone, 477 in CH_3CN, 468 (408) in methanol. Compound $(DMA)Re(CO)_3Cl$ is still soluble in toluene with $\lambda_{max} = 529$ nm.

The iridium(III) compounds, on the other hand, exhibit less intense ligand-to-metal charge transfer (LMCT) bands at the high-energy side of the visible spectrum [25–27]. The absorption energies do not show vary much for the different compounds which suggests the involvement of the Cp* ligand in these transitions.

(Spectro)electrochemistry in the UV–vis region shows similarly stark differences between the Re^{I} and Ir^{III} systems with $DMA^{0/-}$. Whereas the latter is distinguished by the emergence of an intense new band at about 600 nm [14], the rhenium(I) compound shows intensity reduction of the MLCT features between 400 and 500 nm and only very weak features at long wavelengths (Fig. 6). The presence of the $DMA^{\bullet -}$ ligand in both instances is manifest from the very intense band emerging at about 380 nm. The reversible further reduction of $[(DMA)Re(CO)_3Cl]^{\bullet -}$ to the dianion shows the disappearance of this band (Fig. 6).

2.7. Summary

In spite of the seemingly close similarity of the lumazine, alloxazine and pterin heterocycles, the metal complexes of these oligofunctional ligands exhibit a rather diverse spectroscopy, electron-transfer reactivity and even coordination structure. Specifically, we have shown here how the character of the $5d^6$ metal complex fragments, e.g. electrophilic $[IrCp^*Cl]^+$ versus π-electron-rich $Re(CO)_3Cl$, determines the electrochemical response and the charge transfer absorption. Not unexpectedly, the pterins differ significantly from the 2,4-dioxopteridine systems. As shown similarly for amino and nucleic acid ligands, organometallic complex fragments are also suitable probes for coenzymes and their derivatives.

3. Experimental

3.1. Materials

The ligands DML, DMA, PP and MPP were synthesised according to published procedures [18,19]. Complexes $(DML)Re(CO)_3Cl$, $[(DML)IrCp^*Cl](PF_6)$ and $[(DMA)IrCp^*Cl](PF_6)$ have been described previously [12,14]; single crystals of the latter were obtained for

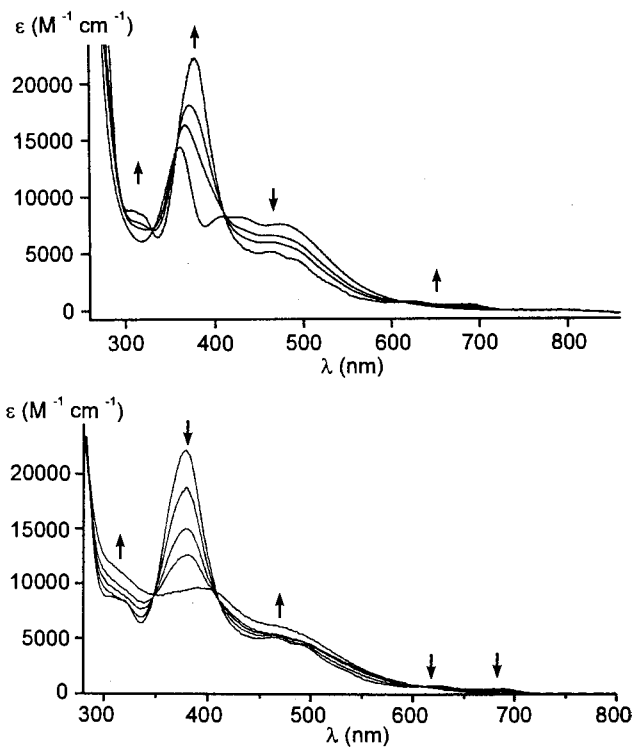

Fig. 6. Spectroelectrochemical response for the transitions $[(DMA)Re(CO)_3Cl]^{(0)\rightarrow(-)}$ (top) and $[(DMA)Re(CO)_3Cl]^{(-)\rightarrow(2-)}$ (bottom) in the UV–vis region (CH_3CN/0.1 M Bu_4NPF_6).

Table 5
Absorption data of ligands and complexes

Compound	λ_{max}(log ε) [a]	Solvent
DMA	319 (3.96), 364sh, 378(4.03), 393sh	THF
[(DMA)Re(CO)$_3$Cl]	363(4.18), 407(3.93), 430(3.91), 477(3.88) [c]	CH_3CN
[(DMA)Re(CO)$_3$Cl]$^{\bullet -}$	308(3.95), 319sh(3.93), 378(4.35), 462(3.72), 490(3.66), 624(2.94), 693(2.77)	CH_3CN
[(DMA)Re(CO)$_3$Cl]$^{2-}$	319sh(4.04), 391(3.99) 472sh(3.79)	CH_3CN
[(DMA)IrCp*Cl]$^+$	359(3.94), 400sh(3.81), 437(3.79), 462sh(3.74)	THF
[(DMA)IrCp*Cl]$^{\bullet}$	315(3.84), 382(3.98), 602(3.74)	THF
DML	320sh, 330(4.02), 344sh	THF
[(DML)Re(CO)$_3$Cl]	459(3.51)	DCE [b] [12]
[(DML)IrCp*Cl]$^+$	353, 389sh, 484	THF [14]
[(DML)IrCp*Cl]$^{\bullet}$	440, 581(3.41)	THF [14]
PP	326(4.01)	THF
[(PP)Re(CO)$_3$Cl]	335sh, 451(3.46)	THF
[(PP–H$^+$)IrCp*Cl]$^+$	350(3.89), 387sh, 455sh	THF
MPP	331 (4.07)	THF
[(MPP)Re(CO)$_3$Cl]	330, 442	THF
	327sh, 449(3.59)	DCE

[a] Absorption maxima λ_{max} in nm, molar extinction coefficients ε in M^{-1} cm^{-1}.
[b] 1,2-Dichloroethane.
[c] Solvatochromic, see text.

X-ray diffraction by slow evaporation of an acetone solution.

3.1.1. (DMA)Re(CO)$_3$Cl

A mixture of 40 mg (0.17 mmol) DMA and 60.7 mg (0.17 mmol) Re(CO)$_5$Cl was heated to reflux for 75 min in 15 ml toluene. The brownish–purple solution was then reduced to about 5 ml and allowed to form a dark-purple precipitate by keeping it at 8°C for 4 days (33 mg, 35%). Anal. Calc. for $C_{15}H_{10}ClN_4O_5Re$ (547.92): C, 32.88; H, 1.63; N, 10.01%. Found: C, 32.90; H, 1.84; N, 10.22%. ^{1}H-NMR (acetone-d_6): $\delta = 3.71$ (s, 3H, N3–CH_3), 3.90 (s, 3H, N1–CH_3), 8.17–8.75 (m, 4H, H6–H9).

3.1.2. (PP)Re(CO)$_3$Cl

A mixture of 69.2 mg (0.28 mmol) PP and 100.0 mg (0.28 mmol) Re(CO)$_5$Cl was heated to reflux for 30 min in 15 ml toluene. The brown solution was reduced by more than half and allowed to form an orange precipitate by keeping it at 8°C for 1 day (121 mg, 78%). Anal. Calc. for $C_{14}H_{13}ClN_5O_5Re$ (552.96): C, 30.41; H, 2.37; N, 12.67%. Found: C, 30.00; H, 2.37; N, 12.11%. ^{1}H-NMR (acetone-d_6): $\delta = 1.44$ (s, 9H, *tert*-Bu–CH_3), 9.18 (d, 1H, H6), 9.24 (d, 1H, H7); $J = 2.6$ Hz; NH signals not observed.

3.1.3. (MPP)Re(CO)$_3$Cl

A solution containing 73.2 mg (0.28 mmol) MPP and 100.0 mg (0.28 mmol) Re(CO)$_5$Cl was heated to reflux for 30 min in 15 ml toluene. The brown solution was reduced by more than half and allowed to form an orange precipitate by keeping it at −30°C for 1 day. Recrystallization from acetone–toluene (1:1) yielded 112 mg (71%) of an orange–brown solid. Anal. Calc. for $C_{15}H_{15}ClN_5O_5Re$ (566.98): C, 31.78; H, 2.67; N, 12.35%. Found: C, 31.04; H, 2.61; N, 11.22%. ^{1}H-NMR (acetone-d_6): $\delta = 1.43$ (s, 9H, *tert*-Bu–CH_3), 3.04 (s, 3H, C6–CH_3), 9.25 (s 1H, H7, 10.76 (br s, 1H, C2–NH), 13.60 (br s, 1H, N3–H).

3.1.4. [(PP–H$^+$)IrCp*](PF$_6$)

A solution of 87.3 mg (0.11 mmol) (IrCp*Cl$_2$)$_2$ in 50 ml acetone was heated with 55.6 mg (0.22 mmol) $AgPF_6$ for 30 min. After filtration from the AgCl precipitate the solution was treated with 54.4 mg (0.22 mmol) PP, dissolved in 15 ml acetone. Heating to reflux for 17 h and removal of the solvent produced 153 mg of a red solid, 100 mg of which were chromatographed on neutral Al_2O_3 with ethanol as eluent. Removal of the solvent and dissolution in dichloromethane gave 43.2 mg (26%) of a red solid as ethanol solvate. Anal. Calc. for $C_{23}H_{33}F_6IrN_5O_3P$ (764.74): C, 36.12; H, 4.35; N, 9.16%. Found: C, 37.83; H, 4.31; N, 9.18%. ^{1}H-NMR (acetone-d_6): $\delta =$ 1.33 (s, 9H, *tert*-Bu–CH_3), 1.77 (s, 15H, Cp*–CH_3), 8.74 (d, 1H, H6), 8.95 (d, 1H, H7); $J = 2.6$ Hz; NH signals not observed.

3.2. Instrumentation

EPR spectra were recorded in the X band on a Bruker System ESP 300 equipped with a Bruker ER035M gaussmeter and a HP 5350B microwave counter. ^{1}H-NMR spectra were taken on a Bruker AC 250 spectrometer, infrared spectra were obtained using a Perkin–Elmer Paragon 1000 PC FTIR instrument. UV–vis/NIR absorption spectra were recorded on Shimadzu UV160 and Bruins Instruments Omega 10 spectrophotometers. Cyclic voltammetry was carried out at 100 mV s^{-1} scan rate in solutions containing 0.1 M Bu_4NPF_6 using a three-electrode configuration (glassy carbon electrode, Pt counter electrode, Ag/AgCl reference) and a PAR 273 potentiostat and function generator. The ferrocene/ferrocenium couple served as internal reference. Spectroelectrochemical measurements were performed using an optically transparent thin-layer electrode (OTTLE) cell [35] for UV–vis spectra and a two-electrode capillary for EPR studies [39].

3.3. Crystal structure analysis

Reddish brown single crystals of [(DMA)IrCp*Cl]-(PF_6) were obtained by slow evaporation from an acetone solution. A crystal of dimensions $0.35 \times 0.3 \times 0.15$ mm was used, all measurements were made with graphite-monochromated Mo–K_α radiation ($\lambda =$ 0.71073 Å) on a Syntex $P2_1$ diffractometer. $C_{22}H_{25}ClF_6IrN_4O_2P$ (750.08 g mol^{-1}), monoclinic $P2_1/n$, $a = 11.763(3)$, $b = 15.428(4)$, $c = 15.059(3)$ Å, $\beta = 105.67°$, $Z = 4$, $V = 2631.3(11)$ Å^3, $D_{calc.} = 1.893$ g cm^{-3}, $3.86° < 2\Theta < 60.04°$; 8166 reflections (6951 independent; $h = -9$ to 16, $k = -1$ to 21, $l = -20$ to 20) were collected at 183 K, 6772 reflections were used for the refinement (335 parameter). $R = 0.0447$ [$I = 2\sigma(I)$], $wR_2 = 0.1097$, GOF = 1.070. An empirical absorption correction (ψ scans) was applied ($\mu = 5.307$ mm^{-1}). The structures were solved via direct methods using the SHELXTL-PLUS program package [40]. Refinement was carried out using SHELXL93 [41] employing full-matrix least-squares methods for F^2. All non-hydrogen atoms were refined anisotropically. The hydrogen atoms were placed in their ideal positions and were allowed to ride on the corresponding carbon atoms, methyl groups were introduced as ideally disordered (rotated by 30°).

4. Supplementary material

Crystallographic data for the structural analysis have been deposited with the Cambridge Crystallographic Data Centre, CCDC no. 115167 for compound [(DMA)IrCp*Cl](PF_6). Copies of this information may be obtained free of charge from: The Director, CCDC, 12 Union Road, Cambridge, CB2 1EZ, UK (Fax: +44-1223-336-033; email: deposit@ccdc.cam.ac.uk or www: http://www.ccdc.cam.ac.uk).

Acknowledgements

This work was supported by Deutsche Forschungsgemeinschaft (DFG) and the Fonds der Chemischen Industrie. A donation of $IrCl_3$ from Degussa AG is gratefully acknowledged.

References

[1] W. Kaim, B. Schwederski, O. Heilmann, F. Hornung, Coord. Chem. Rev. 182 (1999) 323.
[2] S.J.N. Burgmayer, Struct. Bonding (Berlin) 92 (1998) 67.
[3] (a) M.J. Clarke, Comments Inorg. Chem. 3 (1984) 133. (b) M.J. Clarke, Rev. Inorg. Chem. 2 (1980) 27. (c) F. Hueso-Ureña, S.B. Jiménez-Pulido, M.N. Moreno-Carretero, M. Quirós-Olozábal, J.M. Sala-Peregrín, Inorg. Chim. Acta 277 (1998) 103.
[4] (a) W. Beck, R. Krämer, Angew. Chem. 103 (1991) 1492; Angew. Chem. Int. Ed. Engl. 30 (1991) 1467. (b) R. Krämer, K. Polborn, C. Robl, W. Beck, Inorg. Chim. Acta 198 (1992) 415.
[5] K. Severin, R. Bergs, W. Beck, Angew. Chem. 110 (1998) 1722; Angew. Chem. Int. Ed. Engl. 37 (1998) 1634.
[6] H. Chen, M.F. Maestre, R.H. Fish, J. Am. Chem. Soc. 117 (1995) 3631.
[7] D.P. Smith, M.T. Griffin, M.M. Olmstead, M.F. Maestre, R.H. Fish, Inorg. Chem. 32 (1993) 4677.
[8] D.P. Smith, E. Kohen, M.M. Maestre, R.H. Fish, Inorg. Chem. 32 (1993) 4119.
[9] D.P. Smith, M.M. Olmstead, B.C. Noll, M.F. Maestre, R.H. Fish, Organometallics 12 (1993) 593.
[10] D.P. Smith, E. Baralt, B. Morales, M.M. Olmstead, M.F. Maestre, R.H. Fish, J. Am. Chem. Soc. 114 (1992) 10647.
[11] H. Chen, S. Ogo, R.H. Fish, J. Am. Chem. Soc. 118 (1996) 4993.
[12] C. Bessenbacher, C. Vogler, W. Kaim, Inorg. Chem. 28 (1989) 4645.
[13] O. Heilmann, H.-D. Hausen, W. Kaim, Z. Naturforsch. 49b (1994) 1554.
[14] O. Heilmann, F.M. Hornung, W. Kaim, J. Fiedler, J. Chem. Soc. Faraday Trans. 92 (1996) 4233.
[15] J. Selbin, J. Sherrill, C.H. Bigger, Inorg. Chem. 13 (1974) 2544.
[16] (a) J. Lauterwein, P. Hemmerich, J.-M. Lhoste, Inorg. Chem. 14 (1975) 2152. (b) J. Lauterwein, P. Hemmerich, J.-M. Lhoste, Inorg. Chem. 14 (1975) 2161.
[17] K.J. Black, H. Huang, S. High, L. Starks, M. Olson, M.E. McGuire, Inorg. Chem. 32 (1993) 5591.
[18] H. Bredereck, W. Pfleiderer, Chem. Ber. 87 (1954) 1119.
[19] (a) J.R. Russell, C.D. Garner, J.A. Joule, J. Chem. Soc. Perkin Trans. 1 (1992) 1245. (b) E.C. Taylor, P.S. Ray, J. Org. Chem. 52 (1987) 3997.
[20] M.S. Nasir, K.D. Karlin, Q. Chen, J. Zubieta, J. Am. Chem. Soc. 114 (1992) 2246.
[21] W. Kaim, S. Kohlmann, Chem. Phys. Lett. 139 (1987) 365.
[22] W. Kaim, H.E.A. Kramer, C. Vogler, J. Rieker, J. Organomet. Chem. 367 (1989) 107.
[23] W. Kaim, S. Kohlmann, Inorg. Chem. 29 (1990) 2909.
[24] A. Klein, C. Vogler, W. Kaim, Organometallics 15 (1996) 236.
[25] M. Ladwig, W. Kaim, J. Organomet. Chem. 439 (1992) 79.
[26] S. Greulich, W. Kaim, A. Stange, H. Stoll, J. Fiedler, S. Zalis, Inorg. Chem. 35 (1996) 3998.
[27] W. Kaim, R. Reinhardt, E. Waldhör, J. Fiedler, J. Organomet. Chem. 524 (1996) 195.
[28] (a) W.K. Smothers, M.S. Wrighton, J. Am. Chem. Soc. 105 (1983) 1067. (b) B.P. Sullivan, B.M. Bolinger, D. Conrad, W.J. Vining, T.J. Meyer, J. Chem. Soc. Chem. Commun. (1985) 1414. (c) J. Hawecker; J.-M. Lehn, R. Ziessel, Helv. Chim. Acta 69 (1986) 1909. (d) C. Kutal, J. Corbin, G. Ferraudi, Organometallics 6 (1986) 533. (e) S. Van Wallendael, R.J. Shaver, D.P. Rillema, B.J. Yoblinski, M. Stathis, T.F. Guarr, Inorg. Chem. 29 (1990) 1761.
[29] (a) R. Ziessel, J. Am. Chem. Soc. 115 (1993) 118. (b) C. Caix, S. Chardon-Noblat, A. Deronzier, R. Ziessel, J. Electroanal. Chem. 362 (1993) 301. (c) A. Deronzier, J.-C. Moutet, Platinum Met. Rev. 42 (1998) 60.
[30] C. White, A. Yates, P.M. Maitlis, Inorg. Synth. 29 (1992) 228.
[31] (a) T. Kohzuma, H. Masuda, O. Yamauchi, J. Am. Chem. Soc. 111 (1989) 3431. (b) J. Perkinson, S. Brodie, K. Yoon, K. Mosny, P.J. Carroll, T. Vance Morgan, S.J.N. Burgmayer, Inorg. Chem. 30 (1991) 719. (c) M. Mitsumi, J. Toyoda, K. Nakasuji, Inorg. Chem. 34 (1995) 3367.
[32] A. Ehrenberg, P. Hemmerich, F. Müller, W. Pfleiderer, Eur. J. Biochem. 16 (1970) 584.
[33] O. Heilmann, S. Zalis, W. Kaim, unpublished results.
[34] J.A. Weil, J.R. Bolton, J.E. Wertz, Electron Paramagnetic Resonance, Wiley, New York, 1994.

[35] M. Krejcik, M. Danek, F. Hartl, J. Electroanal. Chem. 317 (1991) 179.
[36] W. Kaim, W. Bruns, S. Kohlmann, M. Krejcik, Inorg. Chim. Acta 229 (1995) 143.
[37] C. Bessenbacher, W. Kaim, Z. Anorg. Allg. Chemie 577 (1989) 39.
[38] H. Kunkely, A. Vogler, Z. Naturforsch. 53b (1998) 423.
[39] W. Kaim, S. Ernst, V. Kasack, J. Am. Chem. Soc. 112 (1990) 173.
[40] G.M. Sheldrick, SHELXTL-PLUS: An Integrated System for Solving, Refining and Displaying Crystal Structures form Diffraction Data, Siemens Analytical X-Ray Instruments, Madison, WI, 1989.
[41] G.M. Sheldrick, SHELXL93: Program for Crystal Structure Determination, Universität Göttingen, Göttingen, Germany, 1993.